Validity of the concept of separating primary and scatter dose

Radhe Mohan and Chen-Shou Chui
Department of Medical Physics, Memorial Sloan–Kettering Cancer Center, New York, New York 10021

(Received 23 July 1984; accepted for publication 24 July 1985)

The technique of separating dose into primary and scatter components for calculating photon dose distributions is widely used. The primary and scatter dose models ignore the fact that electrons have a finite range. This may be a good approximation for ^{60}Co photons but not for higher energies. For the latter, the range of electrons may be several centimeters in soft tissue and even longer in lungs and will lead to errors in computed dose in regions where electronic equilibrium does not exist. Ignoring the finite range of electrons will affect dose at points such as those near the beam boundaries, near inhomogeneity boundaries, and at bone–soft-tissue interfaces. Other possible problems associated with the definition and use of "primary" and "scatter" dose in dose distribution calculations result from extrapolation of measured data to obtain data for zero and very large field sizes and from the use of these quantities, which are defined for central axis, for points at large distances from the central axis. This paper examines the limits of the validity of these assumptions.

Key words: dosimetry, dose computation models, scatter–air ratios, electronic equilibrium, scatter integration, scatter dose models

I. INTRODUCTION

The accurate calculation of dose due to a photon beam incident on a medium of arbitrary shape, composition, and structure must incorporate the three-dimensional nature of photon and electron scattering and energy deposition phenomena. The availability of three-dimensional descriptions of internal structure from computed tomography (CT) and nuclear magnetic resonance (NMR) imaging devices provides an opportunity to compute dose in the human body with increased accuracy. It is generally believed that the dose computation models which are based on the separation of dose into primary and scatter components[1–5] have the greatest potential for achieving this goal. However, a number of assumptions are implicit in the definition and application of primary and scatter dose models. The validity of these assumptions is not *a priori* evident and may be questionable, especially for high-energy photon beams.

The primary component of dose is defined as the dose on the axis of zero-area radiation beam. It is assumed to be proportional to zero-area tissue–air ratios (TARs). Zero-area TARs are normally obtained by plotting TARs as a function of field size and extrapolating the curves to zero area. The scatter component of the dose is assumed to be related to scatter–air ratios (SARs). SARs are defined as the differences between the TARs of finite field sizes and the corresponding zero-area (primary) values. [We assume that for high energies, tissue–phantom ratios (TPRs) and scatter–phantom ratios (SPRs) are employed in lieu of TARs and SARs, respectively.] The scatter component may be further divided into differential scatter function such as differential scatter–air ratios (or DSARs).[3,4] DSARs represent contribution to dose on the central axis due to small elements of volume located within the field. They are generally obtained by computing the differences between scatter–air ratios of neighboring field sizes and depths.

The primary component of dose at any point in an inhomogeneous medium is computed using TAR $(\Sigma \rho_i d_i, 0)$ where $\Sigma \rho_i d_i$ is the density-weighted path length along the ray joining source and the point. The scatter component may be computed by integrating SARs or DSARs, weighted by the primary photon intensity, over all volume elements surrounding the point of computation.

The following sections describe the assumptions and approximations implicit in the definition and application of primary and scatter dose models and our attempts, based on measurements and Monte Carlo calculations, to quantify the limits of their validity and their impact on the accuracy of dose calculations. Of major concern is the assumption that electronic equilibrium exists at all points in the body. This assumption is examined in Sec. II. Section III explores the consequences of extrapolating the measured data to obtain zero-area TARs and large-field SARs. Section IV examines the impact of the practice that while the TAR(0) and SAR values are defined on the central axis, they are applied for calculation of dose at all points including those that are far off-axis. The effects of the variation in energy spectrum at points off the central axis as well as oblique incidence will be discussed. To explain the behavior of the primary component of dose near the edges of the collimators and blocks, Cunningham *et al.* have introduced certain arbitrary functions.[2,5,7] Constants appearing in these functions are obtained by fitting the functions to measured data. The validity of this approach will be examined in Sec. V.

II. ASSUMPTION OF ELECTRONIC EQUILIBRIUM

The primary and scatter dose models implicitly assume that the range of electrons ejected by photons is zero and that electronic equilibrium exists at all points. It is implied that the primary (zero-area beam) dose contribution is localized along the path of primary photons and is unaffected by variations in structures not lying on the path joining the source of radiation to the point of computation. While the primary

 0094-2405/85/060726-05$01.20

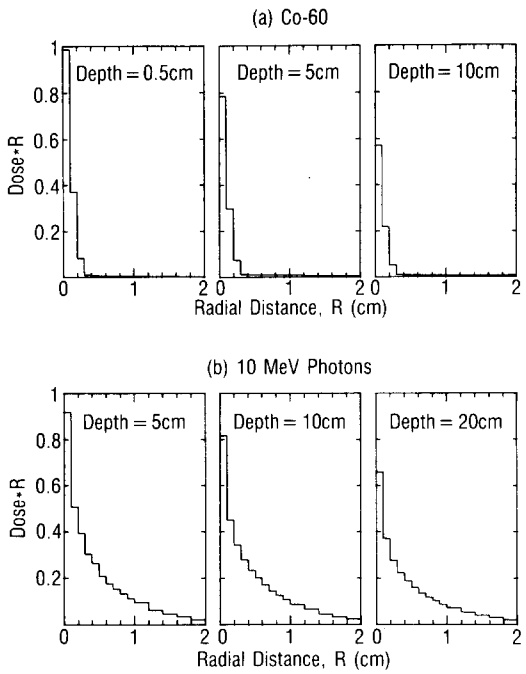

FIG. 1. Dose profiles of zero-area beams of (a) ^{60}Co and (b) 10-MeV monoenergetic photons. Calculations were done using EGS Monte Carlo code (Ref. 8).

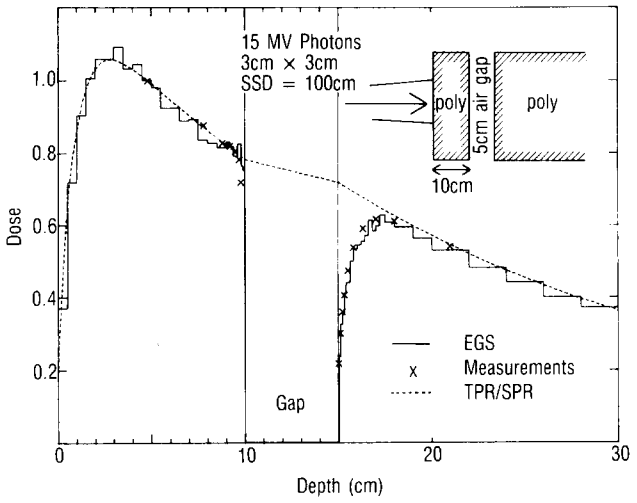

FIG. 2. Effect of loss of equilibrium due to the presence of a gap on a small-field dose distribution. For an infinite field size, the build-down and buildup effects will not be observed. Measurements (×'s) were done using a small thin-window, parallel-plate ionization chamber. Solid line shows the calculations performed with a Monte Carlo code (Ref. 8). Dashed line depicts the estimates based on scatter integration techniques. The dose build-down and buildup effects before and after the gap, respectively, cannot be explained by scatter integration models.

photon intensity at a point is affected only by the structures in the path of the photons, the same is not true of the primary dose. Figure 1 shows Monte Carlo computations of dose profiles at different depths of zero-area beams for ^{60}Co and 10-MeV monoenergetic photons. Energy deposition at a point is mostly due to the electrons ejected by the primary (and scattered) photons at points upstream from it and is a nonlocal and diffuse phenomenon. Electrons travel finite distances, which are sometimes quite large, and deposit a significant fraction of the beam's energy outside the zero-area beam.

Of course, the zero-area beams are not considered in isolation. One could argue that for broad beams the loss of electrons from one part of the beam may be made up by the gain from the neighboring regions. However, the computed dose will be in error in regions where electronic equilibrium is not established. These include points near the beam entrance surface, beam boundaries, and inhomogeneity boundaries. Computed dose will also be in error at points where electronic equilibrium is lost due to the presence of small cavities or structures as well as at interfaces of soft tissue and bone. The following examples illustrate the consequences of ignoring the transport of electrons.

Figure 2 shows measured and calculated values of the central axis depth dose for a small (3×3 cm^2) 15-MV beam incident normally on two slabs of polystyrene separated by a 5-cm gap. The magnitudes of the "build-down" near the exit of the top slab and of the buildup on entry into the bottom slab will increase with decreasing field size and increasing gap. Even for large fields the effect will be significant for points near the beam boundaries. Scatter integration models cannot explain the build-down and buildup behavior. Calculated data shown in Fig. 2 were obtained with the Electron Gamma Shower (EGS) Monte Carlo program[8] (solid line) and estimated with the aid of a scatter integration approach (dashed line). Measured data were obtained with a small (1-cm diameter), thin-window plane parallel-plate chamber.

Electronic equilibrium is also disturbed by the presence of finite cavities and inhomogeneities. Figure 3 shows calculated central axis depth dose data for a 5×5 cm^2 15-MV beam incident normally on a phantom with a cylindrical cavity of height 2 cm and diameter 2 cm. Calculations were performed using the EGS code (solid line) and with an approximate scatter integration method. Build-down and buildup effects are seen although such effects may be quite different for cavities of different sizes.

A hypothetical situation (similar to that shown in Fig. 3) will illustrate the case in point further. Consider a cavity that is vanishingly narrow, say 0.1 cm in diameter, and long, say 5

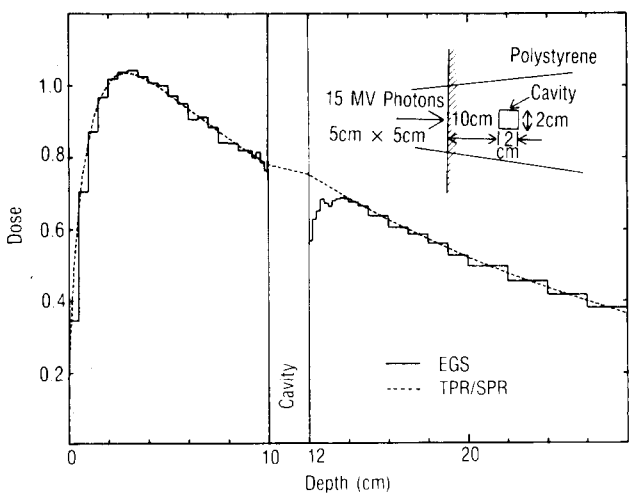

FIG. 3. Monte Carlo calculations illustrating the effect of a cavity of diameter 2 cm and height 2 cm on dose distribution for a 5×5 cm^2 15-MV beam. Scatter integration estimates (dashed line) are also shown.

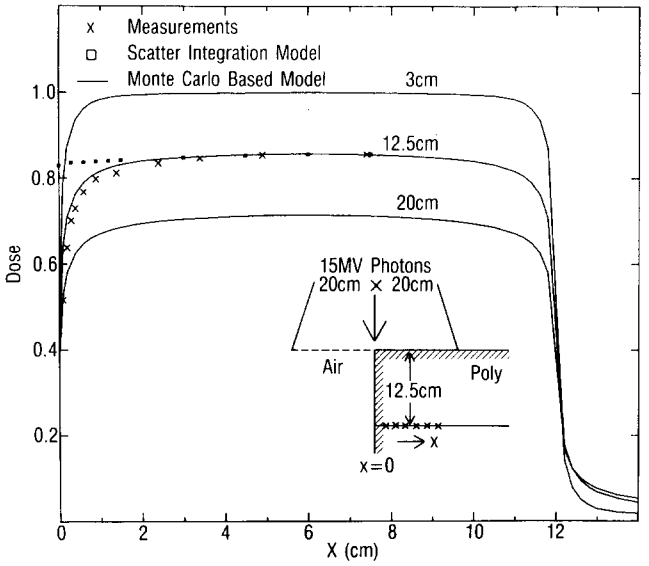

FIG. 4. Beam profiles for a 20×20 cm^2 15-MV beam incident on a quarter-infinite phantom. The central axis is coincident with the vertical face of the phantom. The computations were performed using the scatter integration model (squares) and the model of Ref. 6 (solid line) which takes into account the transport of electrons. The measured data ($\times$'s) were obtained with a small thin-window, parallel-plate chamber positioned parallel to the vertical face of the phantom.

cm. Dose at points just behind the cavity along the beam axis will essentially be the same as if the cavity were filled with water. This can be confirmed by Monte Carlo calculations or by measurements. Conventional dose calculation techniques will predict a much higher dose at these points because of the lack of 5 cm water to attenuate the primary dose. In general, due to the finite range of electrons, the presence of a gap, cavity, or inhomogeneity will affect the dose distribution in a complicated manner. Depending upon the size of the cavity or inhomogeneity, its composition, and its position relative to the beam and other structures, the dose computed by primary and scatter dose models will be underestimated in some instances and overestimated in others.

Another example of the consequences of ignoring the finite range of electrons is given by the plots in Fig. 4 of dose profiles across a 15-MV beam incident normally on a "quarter-infinite" phantom (see inset in Fig. 4). The central axis of the beam is coincident with the vertical face of the phantom. Dose was calculated using a scatter integration model at a number of points at a depth of 12.5 cm. Dose values at depths of 3, 12.5, and 20 cm were also calculated with the "differential pencil beam" (DPB) model, a Monte Carlo based model which incorporates transport of scattered photons and electrons.[6] The latter calculations agree well with ionization chamber measurements. The scatter integration model overestimates the dose at points up to approximately 2 cm from the vertical face. Loss of lateral electronic equilibrium results in a cold spot that cannot be predicted by the scatter integration models.

In short, primary and scatter dose models assume that electronic equilibrium exists. Consequently, the results of dose computations at interfaces, at beam boundaries, at inhomogeneity boundaries, and in regions near small structures may be in significant error due to considerable departures from electronic equilibrium. It should be pointed out that the errors resulting from the assumption of electronic equilibrium are not unique to primary and scatter models. Equivalent path-length methods suffer from similar inadequacies.

III. EXTRAPOLATION OF DATA

The measured data for finite field sizes is extrapolated in order to obtain zero-area TARs. Furthermore, computation of dose at points near and outside the beam boundaries requires SARs of very large field sizes. For example, a point at the corner of 30×30 cm^2 field will require SARs of fields of radii up to 42 cm (or equivalent square of approximately 84×84 cm^2). Field sizes for most machines do not exceed 40×40 cm^2. Therefore, large field size data are also obtained by extrapolation.

In the absence of knowledge of the functional form of the data, extrapolation is an inherently imprecise process resulting in inaccurate separation of primary and scatter. Erroneous small-field data will cause the computed dose to be in error in regions where sudden and significant variations in scatter or primary component occur due to variations in in-

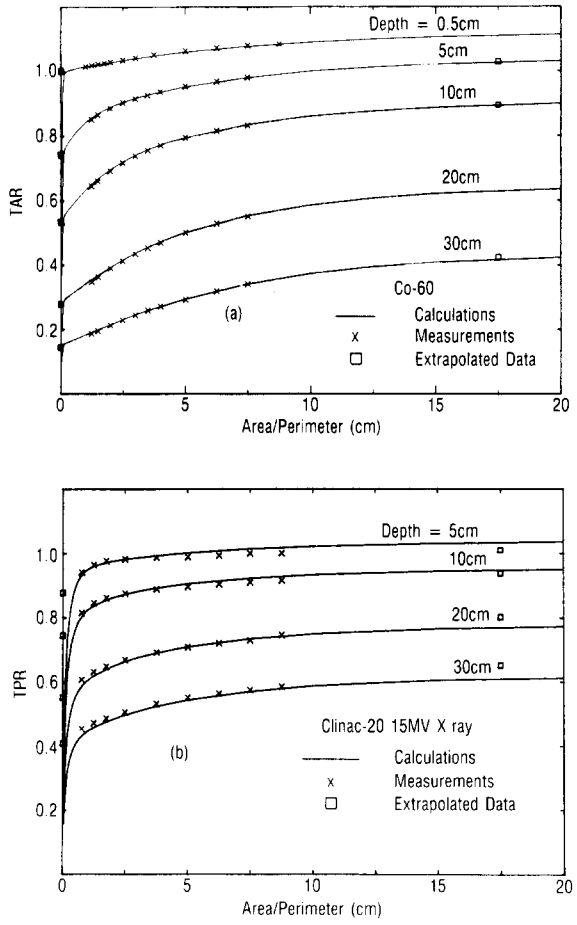

FIG. 5. TPRs/TARs as functions of field size for (a) ^{60}Co and (b) 15-MV photons. Measured data ($\times$'s) are extrapolated to small and large field sizes. Values calculated with the model of Ref. 6 are shown as solid lines. For field sizes smaller than the lateral range of electrons, there is a sudden drop in dose which is not incorporated in the scatter integration models. Consequently, such models will predict incorrect dose near the boundaries of beams, blocks, and inhomogeneities.

ternal structure or surface curvature, or proximity to the beam boundary. Dose near and outside the boundaries of large fields may be in error due to the imprecision in the large-field SARs.

Calculated and measured TAR values for ^{60}Co and the TPR values for 15-MV photons are plotted as a function of area/perimeter in Figs. 5(a) and 5(b). Calculations were performed with the DPB model. For fields smaller than or equal to the lateral range of electrons, the calculated dose drops very suddenly. The corresponding values obtained by extrapolation to zero field sizes are misleadingly high. While it is certain that the actual dose for a zero field size is much smaller than the value obtained by extrapolation of measured data, it is not possible to obtain an accurate estimate of error due to extrapolation with the aid of the Monte Carlo based dose computation model employed. This is due to extremely steep dose gradient at zero field size. Monte Carlo calculation of dose requires the use of a finite scoring region whose size will affect the calculated values of dose deposited in regions of steep gradients.

For the two examples we have chosen, the agreement between the extrapolated data for large fields and the calculations done with the Monte Carlo based model is acceptable.

Comparison of Fig. 5(a) with 5(b) illustrates another interesting point. For field sizes larger than the range of secondary electrons, the TAR (or TPR) curves plotted as functions of field size rise less rapidly for higher energy photons than for ^{60}Co. This indicates that, while scattered photons play a significant role in energy deposition for ^{60}Co fields, they are of lesser importance for higher energies.

For field sizes smaller than the range of secondary electrons, on the other hand, due to the longer range of electrons ejected by higher energy photons, a rapid variation in dose is observed for larger fields for higher energies than for ^{60}Co. In the examples shown, the region of rapid variation for ^{60}Co field sizes is from 0×0 to approximately 0.4×0.4 cm^2. For 15-MV photons, on the other hand, the region of rapid variation extends up to field sizes of approximately 3×3 cm^2. This reemphasizes the fact that in calculating dose for high-energy photons, secondary electrons must also be considered and may play a more important role than scattered photons.

The relative role of scattered photons and secondary electrons is also a factor in two other observed phenomena. Due to a longer range of secondary electrons, the beam profile curves at the beam boundary are much more rounded for say 18-MV photons than for 4-MV photons. On the other hand, due to energy transported by scattered photons, the dose well outside the beam boundary is a higher fraction of the central axis dose for a 4-MV beam than for an 18-MV beam.

IV. USE OF TISSUE–AIR RATIO (0) AND SCATTER–AIR RATIO VALUES AT OFF-AXIS POINTS

Primary and scatter components, and the corresponding TAR(0) and SAR values, are defined on the central axis of a beam incident normally on the surface of a phantom. The phantom surface is more or less uniformly irradiated. The conditions under which primary and scatter components are used in calculating dose at points near and outside the boundaries of large beams may be quite different from the conditions under which they are defined. This may lead to two potential problems.

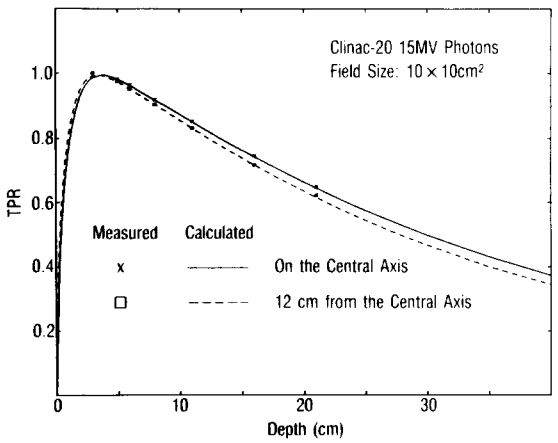

FIG. 6. Tissue–phantom ratios for 15-MV photons for 10×10 cm^2 beam defined at the central axis and a 10×10 cm^2 beam centered 12 cm from the central axis. The differences are due to a shift in energy spectrum from a mean value of 4.1 MeV on the central axis to 3.2 MeV in the region from 10 to 15 cm from the central axis.

First, it is implicitly assumed that the energy spectrum on the central axis and at points off-axis is the same. For linear accelerators this assumption is not valid. Our Monte Carlo calculations for 15-MV photons from a Clinac-20, for example, show that the mean photon energy in the circular region of radius 2 cm around the central axis on the surface of phantom at a distance of 100 cm from the source is 4.1 MeV; whereas the mean energy in an annular region between 10 and 15 cm from the central axis is 3.2 MeV.[9] The measured TPRs used in routine dose calculations correspond approximately to those for an energy spectrum whose mean energy is 4.1 MeV. Figure 6 shows the 10×10 cm^2 TPRs computed using the two different spectra (generated using EGS Monte Carlo code). The difference between the two computations indicates the possibility of up to 10% error at points 10–15 cm off the central axis. Also shown are the measured data obtained in polystyrene for 10×10 cm^2 field sizes defined at the isocenter and at a point 12 cm laterally from the isocenter.

The second problem is that of oblique incidence. The TAR(0) and SAR values obtained for normal incidence are used for points off-axis where scattering conditions are quite different from those on the axis. For example, the ray joining the source with a point lying on the boundary of a 40×40 cm^2 field makes an angle of 10° with the normal. The magnitude of error in dose calculation due to oblique incidence is difficult to estimate. We are simply pointing out a potential source of error.

V. PRIMARY DOSE PROFILES

Empirical functions involving arbitrary constants are often introduced to explain dose distributions near the beam boundaries defined by collimators or blocks.[2,5,7] For certain applications, these functions define an "extended source." The shape of the beam profiles in the medium at the boundaries is due to the following factors: (1) the geometry of the

source, collimating system, and blocks; (2) the photons scattered from the source housing and collimating system; (3) the photons scattered in the medium; and (4) the lateral transport of secondary electrons. The empirical functions cannot properly account for all these factors, especially the lateral transport of electrons.

For ^{60}Co treatment machines, the lateral travel of electrons is of the order of a couple of millimeters and is not an important consideration. The shape of ^{60}Co penumbra is almost entirely due to the other three factors.

For high-energy accelerators, on the other hand, photons scattered from the source housing, collimating system, and the medium play a comparatively less significant role and the lateral transport of electrons is far more important. Our calculations for 15-MV photons show that the contribution of secondary electrons to the formation of a beam penumbra is of the same order of magnitude as the other three factors combined. The right-hand side of the dose profiles in Fig. 4 shows the penumbra resulting from photons scattered in the medium and lateral transport of electrons. The calculations were performed for idealized point sources. Therefore, the effects of source geometry and photon scattering outside the medium have been removed. Since the scattering of 15-MV photons in the medium is relatively small, the penumbra shown is due almost entirely to secondary electrons.

The data shown illustrate that while the extended source analytic function models assume that the beam penumbra shape is formed partly by photons scattered from the collimating systems and partly due to the photons scattered within the medium, in reality the major contributor to the penumbra shape is the lateral transport of electrons. The empirical functions describe the primary dose profiles which are modified slightly by the photon scatter contribution at different depths in the medium. The other three factors are assumed to be included in the empirical functions or the extended source defined by the function. Consequently, their effects on calculations vary monotonically as functions of distance from the source and the lateral distance from the central axis. This is incorrect since the range of secondary electrons is essentially independent of depth and distance from both the source and the central axis. The contribution to the penumbra due to secondary electrons is constant. Thus, for photon energies where secondary electrons contribute significantly to the penumbra, the empirical functions cannot correctly predict dose near the boundaries of beams formed by collimators or blocks.

VI. CONCLUSIONS

A number of questions regarding the assumptions and approximations implicit in the definition of primary and scatter dose and in the procedures involving their use in the calculation of dose have been raised. The most significant of these is that the primary and scatter dose models ignore the effect of the finite range of electrons. The range of electrons in lungs and cavities can be many centimeters for high-energy x rays and must be taken into account for accurate dose calculations. The basic assumption that we can eliminate scatter contribution to dose by reducing the field size to zero is in error. All energy deposition results from the transport of electrons in a complicated manner from the points of collisions of photons and electrons and is affected by variations in structure at points around the point of computation. No component of dose can be assumed to be affected solely by the matter lying on the ray joining the source of radiation and point of computation. All dose deposition phenomena should be considered as resulting from scattering.

There are many additional problems associated with the definition and use of "primary" and "scatter" dose in dose distribution calculations. For example, the extrapolation necessary to obtain data for zero and very large field sizes may introduce uncertainties into the data, although our investigation revealed that this is not important for large fields. Furthermore, the separation of primary and scatter is performed using data on the central axes of the beams. However, the actual points of calculation are not always located on or near the central axes. The results of calculation at points near or outside the beam boundaries, especially for large field sizes, may be in error due to the changing energy spectrum for linear accelerators and due to oblique incidence. Use of empirical functions to account for dose near the boundaries of beams formed by collimators and blocks may also be in error.

It can be argued that the errors resulting from assumptions implicit in the models employing primary and scatter dose concepts are insignificant because we ultimately add up what we separated. We believe this to be an oversimplification, true only for points that are on the central part of the beam, away from boundaries of inhomogeneities and small structures, and only for low-energy photons.

In summary, like other practical models of dose computation, the primary and scatter dose models make assumptions and approximations which limit their accuracy and applicability in a number of situations. We therefore believe that for accurate dose distribution calculations for high-energy photons there is a need for continued development of more accurate models, especially those incorporating the transport of electrons.

ACKNOWLEDGMENT

We are indebted to Mrs. Kathleen C. Podmaniczky for her critical review of this paper and several helpful suggestions.

[1]M. R. Sontag and J. R. Cunningham, Radiology **129**, 787 (1978).
[2]J. R. Cunningham, Phys. Med. Biol **17**, 42 (1972).
[3]K. B. Larson and S. C. Prasad, in *Proceedings of the Second Annual Symposium on Computer Applications in Medical Care, Washington, D. C.* (IEEE Computer Society, New York, 1978), pp. 93–99.
[4]J. R. Cunningham and L. Beaudoin, in Proceedings of the XIII International Congress of Radiology, Madrid, Oct. 15–20, 1973.
[5]H. E. Johns and J. R. Cunningham, *The Physics of Radiology*, 4th ed. (Thomas, Springfield, IL, 1983).
[6]C. S. Chui, R. Mohan, and L. Lidofsky, Med. Phys. **11**, 392 (1984).
[7]J. R. Cunningham, P. N. Shrivastava, and J. M. Wilkinson, Comput. Programs Biomed. **2**, 192 (1972).
[8]R. L. Ford and W. R. Nelson, "The EGS Code. Computer Programs for the Monte Carlo Simulation of Electromagnetic Cascade Showers," SLAC-210, 1978.
[9]R. Mohan and C. Chui, Int. J. Radiat. Oncol. Biol. Phys. **10**, Suppl. 2, 182 (1984).